Biosensors and Bioelectronics 25 (2009) 773–777

Contents lists available at ScienceDirect

Biosensors and Bioelectronics

journal homepage: www.elsevier.com/locate/bios

Three-dimensionally ordered macroporous (3DOM) gold-nanoparticle-doped titanium dioxide (GTD) photonic crystals modified electrodes for hydrogen peroxide biosensor

Jianlin Li[a,*], Tao Han[b], Nannan Wei[b], Jiangyan Du[b,*], Xiangwei Zhao[c]

[a] Department of Food Science and Nutrition, Nanjing Normal University, Nanjing 210097, China
[b] Jiangsu Key Laboratory of Biofunctional Materials,College of Chemistry and Environment, Nanjing Normal University, Nanjing 210097, China
[c] State Key Laboratory of Bioelectronics, Southeast University, Nanjing 210096, China

ARTICLE INFO

Article history:
Received 15 June 2009
Received in revised form 6 August 2009
Accepted 18 August 2009
Available online 25 August 2009

Keywords:
Gold-nanoparticle-doped
Titanium dioxide
Photonic crystals
Horseradish peroxidase
Electrocatalysis

ABSTRACT

Gold nanoparticles have been introduced into the wall framework of titanium dioxide photonic crystals by the colloidal crystal template technique. The three-dimensionally ordered macroporous gold-nanoparticle-doped titanium dioxide (3DOM GTD) film was modified on the indium-tin oxide (ITO) electrode surface and used for the hydrogen peroxide biosensor. The direct electron transfer and electrocatalysis of horseradish peroxidase (HRP) immobilized on this film have been investigated. The 3DOM GTD film could provide a good microenvironment for retaining the biological bioactivity, large internal area, and superior conductivity. The HRP/3DOM GTD/ITO electrode exhibited two couples of redox peaks corresponding to the HRP intercalated in the mesopores and adsorbed on the external surface of the film with the formal potential of −0.19 and −0.52 V in 0.1 M PBS (pH 7.4), respectively. The HRP intercalated in the mesopores showed a surface-controlled process with a single proton transfer. The direct electron transfer between the adsorbed HRP and the electrode is achieved without the aid of an electron mediator. The H_2O_2 biosensor displayed a rapid eletrocatalytic response (less than 3 s), a wide linear range from 0.5 μM to 1.4 mM with a detection limit of 0.2 μM, high sensitivity (179.9 μA mM^{-1}), good stability and reproducibility. Compared with the free-Au doped titanium dioxide photonic crystals modified electrode, the GTD modified electrode could greatly enhance the response current signal, linear detection range and higher sensitivity. The 3DOM GTD provided a new matrix for protein immobilization and direct transfer study and opened a way for low conductivity electrode biosensor.

1. Introduction

The design and fabrication of simply, sensitively electrochemical biosensors have been of high interest for their widespread applications such as drug discovery, disease diagnostics, environmental monitoring and food safety. However, the miniaturization trend of electrochemical biosensors makes the utilization of them still challenging because of the limited active surface area of microelectrodes and the low detection signal. The electrodes modified with multiporous structure were considered as one of effective paths to solve the problem (Ben-Ali et al., 2003, 2005; Privett et al., 2008; Szamocki et al., 2007). These multiporous electrodes have high active surface area and could increase significantly detection signals (Lu and Eychmüller, 2008; Song et al., 2005; Szamocki et al., 2006, 2007). Therefore, electrochemical detection techniques with the modified multiporous electrodes become a focus in the field.

Several techniques have been developed to fabricate the modified multiporous electrodes such as sol–gel techniques (Chen et al., 2006a,b; Yu and Ju, 2002), etching techniques (Liu and Chen, 2005; Xie et al., 2007), template techniques (Ben-Ali et al., 2003, 2005; Lu and Eychmüller, 2008; Song et al., 2005; Szamocki et al., 2006, 2007). Among these methods, three-dimensionally ordered macroporous (3DOM) (>50 nm) modified electrodes fabricated by the template method have recently received great attention because of its simple process, cost effectiveness, controllable sizes of pore and film thickness. Some good biocompatibility materials, such as Au, Ag, TiO_2, SiO_2, C and semiconductor quantum-dot nanoparticles, have usually been used for the modification of multiporous electrodes (Daniel and Astruc, 2004; Katz and Willner, 2004; Lai et al., 2007; Lu and Eychmüller, 2008; Privett et al., 2008; Rosi and Mirkin, 2005). For example, 3DOM gold film modified electrodes have been used for the electrochemical detections of hemoglobin

* Corresponding authors. Tel.: +86 25 83598286; fax: +86 25 83707623.
E-mail addresses: jianlinli82003@yahoo.com.cn (J. Li), dujiangyan@njnu.edu.cn (J. Du).

0956-5663/$ – see front matter © 2009 Elsevier B.V. All rights reserved.
doi:10.1016/j.bios.2009.08.026

(Wang et al., 2005), glucose (Song et al., 2005; Szamocki et al., 2006), nicotinamide adenine dinucleotide (NADH) (Ben-Ali et al., 2003), tripropylamine (Gao et al., 2007), and C-reactive protein (Chen et al., 2008b). Recently, 3DOM TiO_2 film modified electrodes have been reported for immobilization of horseradish peroxidase (HRP) (Zhu et al., 2009). These open, interconnected and periodic 3DOM structures provide a high stability, an increase of up to 2 orders of magnitude active surface area, more than one order of magnitude signal compared to that on a flat electrode (Szamocki et al., 2006, 2007). Among the modified electrodes, the 3DOM TiO_2 film became apparent and fascinating in the electrochemistry field because of its unique properties and wide application in life science, medicinal field, photocatalysis and solar batteries.

The sensitive detection of hydrogen peroxide (H_2O_2) is becoming of practical importance in the clinical, environmental, biological, industrial analysis fields (Bartlett et al., 1998; Chen et al., 2006a,b; Yu and Ju, 2003). Electrochemical methods for H_2O_2 detection have been demonstrated to be a simple, rapid, and inexpensive method. HRP is the most commonly used enzyme for the construction of H_2O_2 biosensor (Chen et al., 2006a,b). However, because the HRP electroactive center is deeply embedded within the glycoprotein, absorptive denaturation and unfavorable orientation, proteins exhibit a rather slow rate of heterogenous electron transfer at a conventional electrode (Rusling, 1998; Zhu et al., 2009). Therefore, it is a challenge to achieve direct electrochemistry of HRP. The high electron transfer rate mainly depends on the proper immobilization conditions of HRP (Ferapontova and Gorton, 2003). Several immobilization strategies and materials have been developed to increase the electron transfer including metal nanoparticles modification (Chen et al., 2006a,b; Ferapontova and Gorton, 2003; Jia et al., 2007; Yuan et al., 2008), covalent and affinity binding modification, surfactant and layer-by-layer films modification, multiporous modification electrodes (Leĭger and Bertrand, 2008).

Colloidal gold nanoparticles have been widely used as an immobilized matrix for retaining the bioactivity of biomolecules. Recently, colloidal gold nanoparticles/TiO_2 composite architecture exhibited to promote the direct electron transfer of the immobilized proteins (Chen et al., 2006a,b; Guerin et al., 2006; Shi et al., 2007). In our previous work, we designed a new label-free immunosensor and chemical sensor based on the 3DOM TiO_2 photonic crystals film by the optical spectrometers. This 3DOM TiO_2 photonic crystals film showed a good biocompatibility, high sensitivity and unique optical properties (Li et al., 2008; Li and Zheng, 2008). Recently, we fabricated a new 3DOM gold-nanoparticle-doped titanium dioxide (GTD) photonic crystals modified electrode by the colloidal crystal template technique (Han et al., submitted). The scanning electron microscope (SEM) image shows that the film is face-centered cubic ordered hexagonal network structure and the gold nanoparticles are introduced within the framework (Fig. 1). The hexagonal networks stack layer-by-layer forming a 3DOM periodical structure with the interpenetrated pores.

In this paper, using the 3DOM GTD/indium-tin oxide (ITO) electrode, we developed a new HRP-based H_2O_2 biosensor. It is first report on the 3DOM GTD/ITO electrode for biosensor for direct electrochemistry of HRP. This 3DOM modified electrodes can ensure the accessibility of reactants to the surface active sites of electrodes, increasing both the mass transport of reactant and mass-normalized activity. The influence factors of responsive current intensity were discussed. The quantitative relationship between the responsive current intensity and H_2O_2 concentration was established. This novel H_2O_2 biosensor displayed high sensitivity, acceptable stability and reproducibility. These provide a fundamental theory principle for the new biosensor application.

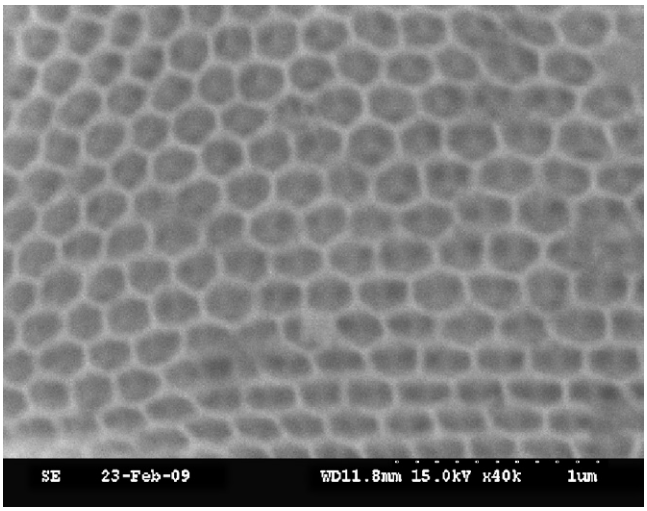

Fig. 1. The SEM of the 3DOM GTD photonic crystals modified electrode.

2. Experimental

2.1. Reagents

HRP (EC 1.11.17, RZ > 3.0, A > 300 units/mg) was bought from Sigma chemical. Titanium (IV) butoxide, H_2O_2 (30%) and ethanol absolute were purchased from Chemical Reagents Co., Ltd. of China. Triethanolamine (TEA), $HAuCl_4$ were from the Nanjing Sunshine Biotechnology Ltd., China. The water was Milli-Q water at 18 MΩ. All other chemicals were of analytical grade and were used without further purification. ITO glasses (<20 Ω/cm^2) were purchased from Wuxi Kang Li Electron Industry Co., Ltd of China. The diameter 290 ± 15 nm polystyrene (PS) microspheres were synthesized in our laboratory.

2.2. Substrate preparation

The preparation of 3DOM GTD photonic crystals was performed by the colloidal crystal template method (Han et al., submitted). GTD sol–gel solution was synthesized by mixture of ethanol absolute, TEA, titanium (IV) butoxide, $HAuCl_4$, and deionized water at 0.3:1:0.5:3 volume ratios under constant stirring until a red wine color solution appeared at room temperature. ITO glasses were cleaned 3 times with deionized water. The cleaned ITO substrates were immersed into 0.2% (v/v_0) colloidal suspension of PS microspheres for 48 h at the room temperature. The PS template substrates were fixed at 95 °C for 1 h. The interspaces of PS opal template were infiltrated with GTD colloids solution through the dip-coating method. After the sample was dried, the infiltrations were repeated 3 times to ensure that the voids in the template were sufficiently filled. The film was calcined in the oven at 500 °C to remove the template. The temperature of the oven was raised from 25 °C to 500 °C at speed of 2 °C/min, and then descended from 500 °C to 25 °C at speed of 2 °C/min. The ITO substrates modified with GTD photonic crystals were cut at 1 cm × 1 cm area.

2.3. HRP immobilization

The 3DOM GTD/ITO electrode was cleaned 2 times with ethanol absolute. For preparation of a HRP electrode, 3DOM GTD/ITO electrode was immersed in 0.1 M pH 7.4 phosphate buffer solution (PBS) containing 0.2 mg/mL HRP at 4 °C for 24 h. Before electrochemical experiments, the electrode was rinsed thoroughly with doubly dis-

tilled water to remove unbound HRP and kept in PBS at 4 °C when not in use.

2.4. Electrochemical detection of H_2O_2

Electrochemical measurements were carried out with M273 electrochemical workstation (EG&G Co., USA). A three-electrode cell was used comprising a saturated calomel electrode (SCE) as reference electrode, a platinum wire as auxiliary electrode, and HRP/3DOM GTD/ITO as working electrode. Cyclic voltammetry (CV) measurements were performed in a 10 mL electrochemical cell at 25 ± 0.2 °C. Prior to the electrochemical measurements, buffers were purged with highly pure nitrogen for 15 min and a nitrogen atmosphere was kept over the solutions during the electrochemical measurements. Aliquots of a standard solution of H_2O_2 were successively added to the cell.

3. Results and discussion

3.1. Cyclic voltammetry behavior of the 3DOM GTD modified electrode

Fig. 2 shows the CVs of the differently modified electrodes in the 0.1 M PBS (pH 7.4). In the absence of HRP, no signals of the ITO and 3DOM GTD/ITO electrode were observed (Fig. 1a and b). In contrast, HRP/3DOM GTD/ITO electrode shows two couples of well-defined redox peaks appear at −0.24 V and −0.05 V for the first couple and −0.57 V and −0.47 V for another couple, respectively. The peak-to-peak separations of the two couples of redox peak were 0.19 V and 0.1 V, respectively. Comparing with the two strong reduction peaks, the two oxidation peaks were rather weak. This resulted from the large band gap (3.2 eV) for this nanoporous material at higher potential (Topoglidis et al., 2001a,b). The similar results were also reported in the studies of immobilized cytochrome c and HRP on nanoporous TiO_2 films (Liu and Chen, 2005; Topoglidis et al., 2001a,b). The two couples of redox peaks of HRP have also been observed on the hexagonal mesoporous silica (Dai et al., 2005) and mercaptopropionic acid modified electrodes (Li and Dong, 1997), which come from the two states of the immobilized HRP. The couple of redox peaks occurring at lower potential were assigned to the redox of HRP intercalated in the mesopores, and another couple of redox peaks resulted from oxidation and reduction of the HRP adsorbed on the external surface of the mesoporous structure

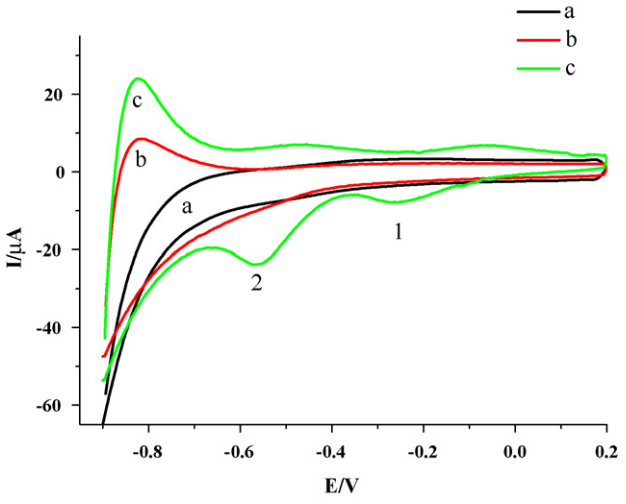

Fig. 2. CVs of the differently modified electrode in 0.1 M PBS (pH 7.4) at 100 mV/s scan rate. (a) ITO electrode, (b) 3DOM GTD/ITO electrode, and (c) HRP/3DOM GTD/ITO electrode.

by physical adsorption (Dai et al., 2005). These HRP intercalated in the mesopores have been demonstrated by the Fourier transform infrared (FTIR) spectra and N_2 adsorption isotherms experiments (Dai et al., 2005). This indicated that the oxidation of HRP undergoes two distinctly separated one-electron processes. Our fabricated macroporous structure with 260 nm diameter is large enough to allow infiltration of HRP into the modified electrode. Therefore, HRP can be adsorbed not only on the external surface but also on the internal surface of 3DOM structure. This result was also demonstrated by our previous study (Li et al., 2008). In addition, the reduction peak signal of the lower potential (reduction peak 2) was stronger than that of the higher potential (reduction peak 1) (Fig. 2c). This might result from two reasons. One is more HRP molecules immobilized on the internal surface than that of the external surface of 3DOM structure. Another reason is the large band gap for this nanoporous material at higher potential. This 3DOM photonic crystals structure can provide a larger than 27 m^2/cm^3 internal surface area, which was remarkably larger than that of the external surface (Li et al., 2008). This makes the reduction current (reduction peak 2) almost reach to 30 μA without help of mediator molecules. From Fig. 2, the 3DOM GTD/ITO electrode has a low background signal. These indicate that the direct electron transfer of HRP can be achieved on the 3DOM GTD/ITO electrode and our fabrication electrode is a good microenvironment for HRP immobilization.

3.2. Electrochemical properties of HRP in the 3DOM GTD/ITO electrode

Fig. 3A shows the CVs of the HRP immobilized electrode at different scan rates in 0.1 M PBS (pH 7.4) solution. The scan rates from "a" to "f" are 50 mV/s, 100 mV/s, 200 mV/s, 300 mV/s, 400 mV/s, and 500 mV/s, respectively. It can be seen that both the peak-to-peak separation and redox peak currents increased with increasing scan rate and the reduction peak position produced a negative shift and oxidation peak position produced a positive shift. Fig. 3B shows the relationship between the scan rates and redox peak currents. The peak currents vary linearly with the scan rates. This indicates the electrochemical behavior of HRP/3DOM GTD/ITO electrode is a surface-controlled process, as expected for an immobilized system. The maximum peak-to-peak separations of lower and higher potentials are 0.158 V and 0.256 V, respectively. According to Laviron formula (Laviron, 1979), when the peak-to-peak separation is less than 200 mV, the peak current $Ip = nFQv/4RT$ (n is the number of transfer electron and Q is the quantity of charge), n can be calculated to be 0.91 ± 0.03. The electrode transfer rate constant can be calculated with the formula $Ks = mnFv/RT$, where m is a parameter related to the peak-to-peak separation. From the Fig. 3 data, The Ks value in this study is obtained to be 0.974 ± 0.05 s^{-1}, which is larger than 0.66 s^{-1} on the graphite electrode (Ruzgas et al., 1995; Zhang et al., 2004) and 0.72 s^{-1} on the regenerated silk fibroin film (Wu et al., 2006). The results demonstrate the 3DOM GTD structure could enhance the electron transfer rate.

3.3. Effect of pH on direct electron transfer of HRP/3DOM GTD/ITO electrode

The effect of solution pH on the response of HRP/3DOM GTD/ITO electrode has been investigated (Fig. 4). From Fig. 4, the peak currents of the direct electrochemistry immobilized HRP are strongly dependent on solution pH. The reduction peak current of low potential peak increases with increasing solution pH from 5.5 to 7.5 and reaches the maximum peak current around pH 7.5. The peak currents of the redox peaks both the reduction and oxidation produced a negative shift as increasing pH. When the solution pH is over 7.5, the reduction peak current of low potential peak

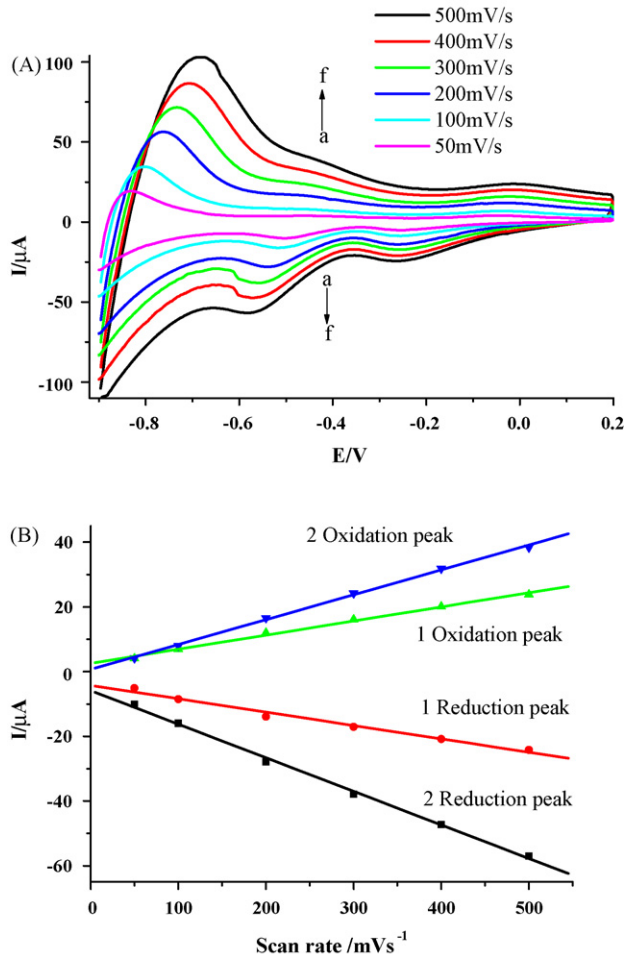

Fig. 3. The influence of scan rates on the response of HRP/3DOM GTD/ITO electrode. (A) CVs of HRP/3DOM GTD/ITO electrode in 0.1 M PBS (pH 7.4) at different scan rates. (B) The relationship between the peak currents and the scan rates.

remarkably decreases. The optimum pH for the low potential peak is in agreement with that of the previous report (Kong et al., 2003). It is known that the peak current is directly related to the amount of HRP adsorbed on the electrode and the adsorbed amount of HRP would reach to a maximum value at the isoelectric point (p*I*) of HRP. The optimum pH is very close to the p*I* of HRP 7.2. In addition, the TiO_2 surface is negatively charged above pH ~ 6.2 solution (Topoglidis et al., 2001a). HRP is also negatively charged above pH 7.5 solution. Consequently, the adsorbed amount of HRP would reduce and peak current decrease when the pH solution is above 7.5. Therefore, solution pH 7.4 was selected for the following study. The formal potential E^0 has a linear relationship with pH value and the slope is −54.51 mV/pH which is close to the theoretical value of −58.0 mV/pH for a single proton transfer coupled to reversible single electron transfer (Fig. 4). This indicates that the diffusion of proton participating in the electron transfer process is rather fast in the 3DOM GTD structure.

3.4. Electrochemical response of the immobilized HRP to H_2O_2

Fig. 5 shows CVs of the HRP/3DOM GTD/ITO electrode recorded in 0.1 MPBS at pH 7.4 in the successive addition of 0.2 M H_2O_2 at 100 mV/s. With increasing H_2O_2 concentration, the reduction peak currents of low potential peak increase significantly. However, the reduction peak currents of higher potential peak decrease and even disappear in the high concentration of H_2O_2. This is attributed to the different formal potentials of the two couples of redox peak which are −0.52 and −0.15 V at the lower and higher potential, respectively (Fig. 2). The formal potential of the HRP intercalated in the mesopores at the lower potential is close to −0.46 V of native HRP in solution (Dai et al., 2005; Harbury, 1957) and the HRP at the lower potential is easy to be oxidized. In addition, no direct reduction peak was observed at HRP-free/3DOM GTD/ITO electrode in the presence of H_2O_2. Thus, the reduction peak current changes result from the reaction of HRP with H_2O_2. It was noticeable that the oxidation peaks have disappeared in the higher concentration H_2O_2. This indicates that the oxidation rate of HRP by H_2O_2 is rather fast. Fig. 6 exhibits the relationship between the H_2O_2 concentration and reduction peak currents under the condition of continuous addition of aliquot of H_2O_2 to the buffer solution. It can be seen that reduction peak current values increased linearly with the concentration of H_2O_2 from 0.5 μM to 1.4 mM with a correlation coefficient of 0.9989 (n = 26). The detection limit is 0.2 μM for a signal-to-noise ratio of 3. In the linear range, the biosensor has a high sensitivity of 179.9 μA mM^{-1}, which is higher than those of 120.2 μA mM^{-1} for HRP on chitosan/carbon microsphere (Chen et al., 2008a), 102.9 μA mM^{-1} for H_2O_2 detection under UV light on 3DOM TiO_2 photonic crystals (Zhu et al., 2009) and 61.5 μA mM^{-1} on porous titania sol–gel matrix (Yu and Ju, 2002). We also compared the electrochemical response of HRP/TiO_2 photonic crystal/ITO electrode with HRP/3DOM GTD/ITO electrode to H_2O_2 in pH 7.4 PBS solution (Fig. 6). Obviously, the HRP/3DOM

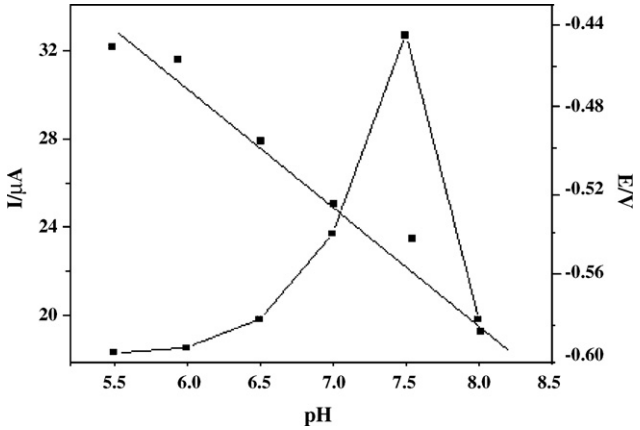

Fig. 4. The effect of solution pH on the response HRP/3DOM GTD/ITO electrode and formal potential.

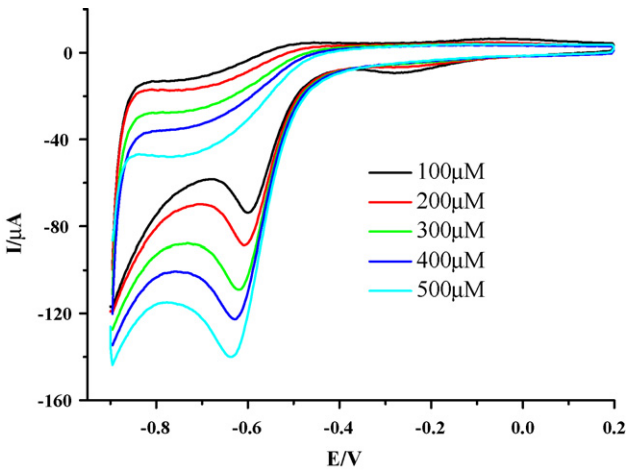

Fig. 5. CVs of HRP/3DOM GTD/ITO in 0.1 M PBS (pH 7.4) containing different concentration of H_2O_2 at 100 mV/s scan rate.

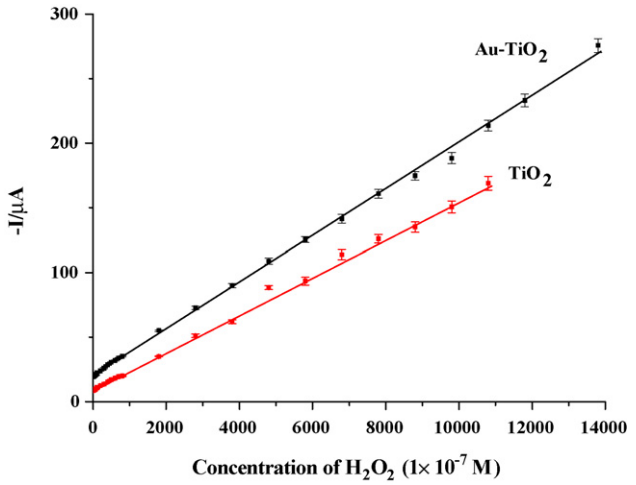

Fig. 6. The relationship between the concentration H_2O_2 and the reduction peak currents.

GTD/ITO electrode has wider linear detection range, higher sensitivity and higher response peak current to the same concentration of H_2O_2 than that of HRP/TiO_2 photonic crystal/ITO electrode. Gold nanoparticles doped into the framework could enhance the conductivity of this film and promote the direct electron transfer of the immobilized proteins. This result is in agreement with the previous reports (Chen et al., 2006a,b; Guerin et al., 2006; Shi et al., 2007). In addition, the response time of the electrode to H_2O_2 is less than 3 s. The high sensitivity, wide detection range and fast response are assigned to the high mass transport of reactant and high reactive enzyme loading.

3.5. Reproducibility and stability of the HRP/3DOM GTD/ITO electrode

The stability of this biosensor was investigated when the HRP/3DOM GTD/ITO electrode was stored in PBS in a refrigerator at 4 °C. No obvious decrease in the response currents to H_2O_2 was observed after one month storage. It retained 90% of its initial current response after six months storage, showing good storage stability. The repeatability of the current response of HRP/3DOM GTD/ITO electrode to 50 μM H_2O_2 was examined. The relative standard deviation (RSD) is 5.3% for six successive determinations. The electrode-to-electrode reproducibility was determined from the four independent electrodes, showing an acceptable reproducibility with a RSD of 8.6% for the current response to 50 μM H_2O_2. The long-term stability and good reproducibility could be attributed to the fact that HRP molecules were strongly attached to the Au modified electrode surface (Radi et al., 2008).

4. Conclusion

In this work, a new HRP-based H_2O_2 biosensor was developed by the 3DOM GTD/ITO electrode. This 3DOM modified electrodes can display the good biocompatibility, large internal area and uniform ordered structure. The immobilized HRP exhibited a catalytic activity and fast response to H_2O_2 without the help of an electron mediator. The developed HRP-based H_2O_2 biosensor has a wide detection range, high sensitivity, long-term stability and acceptable reproducibility. The high electrical activity of the TiO_2 photonic crystal film was attributed to the presence of Au introduced into the 3DOM. The 3DOM GTD film is also used to immobilize other enzymes and other bioactive molecules, providing a new biosensors platform.

Acknowledgments

This work was supported by the project of the National High Technology Research and Development Program of China (863Program) No. 2008AA10Z416, the project of the Natural Science Foundation of the Jiangsu Higher Education Institution of China Nos. 07KJB550058 and 06KJB150054, and the open fund of State Key Laboratory of Bioelectronics of China.

Appendix A. Supplementary data

Supplementary data associated with this article can be found, in the online version, at doi:10.1016/j.bios.2009.08.026.

References

Bartlett, P.N., Birkin, P.R., Wang, J.H., Palmisano, F., Benedetto, G.D., 1998. Anal. Chem. 70, 3685.
Ben-Ali, S., Cook, D.A., Bartlett, P.N., Kuhn, A., 2005. J. Electroanal. Chem. 579, 181–187.
Ben-Ali, S., Cook, D.A., Evans, S.A.G., Thienpont, A., Bartlett, P.N., Kuhn, A., 2003. Electrochem. Commun. 5, 747–751.
Chen, J., Tang, J.H., Yan, F., Ju, H.X., 2006a. Biomaterials 27, 2313–2321.
Chen, S.H., Yuan, R., Chai, Y.Q., Xu, L., Wang, N., Li, X.N., Zhang, L.Y., 2006b. Electroanalysis 18, 471–477.
Chen, X., Li, C.C., Liu, Y.L., Du, Z.F., Xu, S.J., Li, L.M., Zhang, M., Wang, T.H., 2008a. Talanta 77, 37–41.
Chen, X.J., Wang, Y.Y., Zhou, J.J., Yan, W., Li, X.H., Zhu, J.J., 2008b. Anal. Chem. 80, 2133–2140.
Dai, Z.h., Ju, H.x., Chen, H.Y., 2005. Electroanalysis 17, 862–868.
Daniel, M.C., Astruc, D., 2004. Chem. Rev. 104, 293–346.
Ferapontova, E., Gorton, L., 2003. Electroanalysis 15, 484–491.
Gao, W., Xia, X.H., Xu, J.J., Chen, H.Y., 2007. J. Phys. Chem. C 111, 12213–12219.
Guerin, S., Hayden, B.E., Pletcher, D., Rendall, M.E., Suchsland, J.P., Williams, L.J., 2006. J. Comb. Chem. 8, 791–798.
Han, T., Li, J.L., Wei, N.N., Li, Y.W., Du, J.Y. Thin Solid Films, submitted.
Harbury, H.A., 1957. J. Biol. Chem. 225, 1009–1024.
Jia, F.L., Yu, C.F., Ai, Z.H., Zhang, L.Z., 2007. Chem. Mater. 19, 3648–3653.
Katz, E., Willner, I., 2004. Angew. Chem. Int. Ed. 43, 6042–6108.
Kong, Y.T., Boopathi, M.N., Shim, Y.B., 2003. Biosens. Bioelectron. 19, 227–232.
Lai, C.Z., Fierke, M.A., Stein, A., Bühlmann, P., 2007. Anal. Chem. 79, 4621–4626.
Laviron, E., 1979. J. Electroanal. Chem. 101, 19–28.
Leĭger, C., Bertrand, P., 2008. Chem. Rev. 108, 2379–2438.
Li, J.L., Zhao, X.W., Wei, H.M., Gu, Z.Z., Lu, Z.H., 2008. Anal. Chim. Acta 625, 63–69.
Li, J.L., Zheng, T.S., 2008. Sens. Actuators B 131, 190–195.
Li, J.H., Dong, S.J., 1997. J. Electroanal. Chem. 431, 19–22.
Liu, S.Q., Chen, A.C., 2005. Langmuir 21, 8409–8413.
Lu, L.H., Eychmüller, A., 2008. Acc. Chem. Res. 41, 244–253.
Privett, B.J., Shin, J.H., Schoenfisch, M.H., 2008. Anal. Chem. 80, 4499–4517.
Radi, A.E., Lates, V., Marty, J.L., 2008. Electroanalysis 20, 2557–2562.
Rosi, N.L., Mirkin, C.A., 2005. Chem. Rev. 105, 1547–1562.
Rusling, J.F., 1998. Acc. Chem. Res. 31, 363.
Ruzgas, T., Gorton, L., Emneĭus, J.G., Varga, M., 1995. J. Electroanal. Chem. 391, 41–49.
Shi, Y.T., Yuan, R., Chai, Y.Q., He, X.L., 2007. Electrochim. Acta 52, 3518–3524.
Song, Y.Y., Zhang, D., Gao, W., Xia, X.H., 2005. Chem. Eur. J. 11, 2177–2182.
Szamocki, R., Reculusa, S., Ravaine, S., Bartlett, P.N., Kuhn, A., Hempelmann, R., 2006. Angew. Chem. Int. Ed. 45, 1317–1321.
Szamocki, R., Velichko, A., Holzapfel, C., Mücklich, F., Ravaine, S., Garrigue, P., Sojic, N., Hempelmann, R., Kuhn, A., 2007. Anal. Chem. 79, 533–539.
Topoglidis, E., Campbell, C.J., Cass, A.E.G., Durrant, J.R., 2001a. Langmuir 17, 7899–7906.
Topoglidis, E., Cass, A.E.G., O'Regan, B., Durrant, J.R., 2001b. J. Electroanal. Chem. 517, 20–27.
Wang, C.H., Yang, C., Song, Y.Y., Gao, W., Xia, X.H., 2005. Adv. Funct. Mater. 15, 1267–1275.
Wu, Y.H., Shen, Q.C., Hu, S.S., 2006. Anal. Chim. Acta 558, 179–186.
Xie, Y.B., Zhou, L.M., Huang, H.T., 2007. Biosens. Bioelectron. 22, 2812–2818.
Yu, J.H., Ju, H.X., 2002. Anal. Chem. 74, 3579–3583.
Yu, J.H., Ju, H.X., 2003. Anal. Chim. Acta 486, 209–216.
Yuan, P.X., Zhuo, Y., Chai, Y.Q., Ju, H.X., 2008. Electroanalysis 20, 1839–1844.
Zhang, Y., He, P.L., Hu, N.F., 2004. Electrochim. Acta 49, 1981–1988.
Zhu, Y.H., Cao, H.M., Tang, L.H., Yang, X.L., Li, C.Z., 2009. Electrochim. Acta 54, 2823–2827.